Published in final edited form as:

ACS Chem Biol. 2017 March 17; 12(3): 795–804. doi:10.1021/acschembio.6b01006.

Highly-constrained bicyclic scaffolds for the discovery of protease-stable peptides via mRNA display

David E. Hacker[a], **Jan Hoinka**[b], **Emil S. Iqbal**[a], **Teresa M. Przytycka**[b], and **Matthew C.T. Hartman**[a,*]

[a]Virginia Commonwealth University, Department of Chemistry, 1001 West Main Street, Richmond, Virginia 23284-2006, United States

[b]National Center for Biotechnology Information, 8600 Rockville Pike, Bethesda, Maryland 20894, United States

Abstract

Highly-constrained peptides such as the knotted peptide natural products are promising medicinal agents because of their impressive biostability and potent activity. Yet, libraries of highly-constrained peptides are challenging to prepare. Here we present a method which utilizes two robust, orthogonal chemical steps to create highly-constrained bicyclic peptide libraries. This technology was optimized to be compatible with in vitro selections by mRNA display. We performed side-by-side monocyclic and bicyclic selections against a model protein (streptavidin). Both selections resulted in peptides with mid nM affinity, and the bicyclic selection yielded a peptide with remarkable protease resistance.

Introduction

Many bona fide therapeutic targets involve protein-protein interactions. While peptides are attractive candidates for blocking these interactions, they have several drawbacks that have thus far limited wide-scale clinical application, chief among them being low bio-stability and lack of cell permeability. Cyclization of peptides has been shown to increase protease resistance,[1, 2, 3, 4, 5] and as a result many techniques have been used to create these macrocyclic peptides.[6] Cyclization[7] has also been shown to lead to improved target affinity, [8, 9, 10, 11] specificity,[12, 13] and cell permeability.[14, 15, 16, 17] Introduction of a second macrocycle into a peptide is particularly advantageous and has been shown to further increase both target affinity[18, 19] and bio-stability[11, 20] and cell permeability[21, 22, 23] relative to the linear and monocyclic versions. Highly-constrained bicyclic peptides are similar to the highly potent knotted peptide natural products, an attractive and emerging class of therapeutics with enhanced stability and bioavailability derived from their knotted structures.[24, 25, 26] Knotted peptides and miniproteins have displayed a wide scope of

* mchartman@vcu.edu.

Supporting Information

Supporting Tables S1–S6 and Supporting Figures S1–S12, details on materials, reagents and reagent preparation, *in vitro* peptide synthesis and purification, and DNA sequencing and sequence analysis can be found in the Supporting Information associated with this publication. This material is available free of charge via the Internet at http://pubs.acs.org.

biological activities, including uses as antimicrobials,[27, 28] protease inhibitors[29, 30] and as highly potent modulators of a variety of ion channels.[31, 32, 33] Furthermore, knotted peptides and peptide conjugates have been adapted for use as imaging agents [34, 35] and drug delivery vehicles [36].

While knotted peptides have exciting potential in these and other applications, difficulties in synthesis have limited access to large libraries of these constrained peptides. In general, cyclization reactions for creation of highly-constrained peptide libraries must be: (1) robust and high-yielding to maximize enrichment, (2) mild enough to be compatible within the selection system used for ligand discovery, and (3) orthogonal to prevent synthesis of complicated, isomeric cyclic mixtures. Research focused on phage display has led to the development of a few cyclization linkers that meet these criteria. The use of 1,3,5-trisbromomethylbenzene (TBMB)[37] to generate bicyclic phage displayed libraries has been used to develop high affinity ligands specific for human plasma kallikrein[38] and human urokinase-type plasminogen activator[18, 39]. Similar strategies involving 1,3,5-triacryloyl-1,3,5-triazinane (TATA) and *N*,*N*′,*N*″-(benzene-1,3,5-triyl)-tris(2-bromoacetamide) (TBAB) have also been reported [40]. While the size of each macrocycle can be varied using these linkers, conformations are limited to two independent loops because of the reliance on a central, trisubstituted linker. In addition, the formation of bicyclic peptides with disulfide bond linkages has been reported,[11, 41, 42] but with this strategy comes the risk of intracellular reductive cleavage that destroys the rings.[43, 44]

Herein we describe the development of a new strategy for making >10^{13} member libraries of highly-constrained bicyclic peptides with precisely directable topologies using mRNA display.[45, 46] Unlike the previous approaches, we have utilized two orthogonal cyclization steps which allow us to create theta-bridged bicyclic peptide libraries in which the size of the 3 loops can be varied. We have used these libraries to find high-affinity mono- and bicyclic binders to a model target, streptavidin.

Results and Discussion

We designed our bicyclization strategy around using two orthogonal cyclization chemistries. The advantage of this strategy is that the attachment points for each loop are independent, and this allows for the creation of either manacle or theta-bridged[47] bicyclic peptides (Figure 1a). The two chemistries we pursued for this purpose were the bis-bromomethyl benzene cysteine alkylation[37] (Figure S1a) and copper-mediated azide-alkyne cycloaddition (CuAAC-Figure S1b).[48, 49] Both cysteine alkylation and CuAAC have been used together on in vitro translated peptides,[49] but they have not been used in tandem for the generation of peptide libraries.

Ribosomal incorporation of ‘clickable’ amino acids

In order to utilize CuAAC cyclization with our peptide libraries, it is necessary to incorporate α-amino acids bearing an azide and an alkyne. We and others have previously shown that L-β-azidohomoalanine (AzHA) and *p*-ethynyl-L-phenylalanine (F-yne, Figure 1b) act as substrates for aminoacylation onto their cognate tRNAs by methionyl-tRNA synthetase (MetRS) and a mutant phenylalanyl-tRNA synthetase (PheRS A294G),

respectively, and can be incorporated independently into peptides in the absence of the wild-type amino acids.[50, 51, 52, 53, 54] To demonstrate the compatibility of click and the cysteine bis-alkylation cyclization methods and to optimize conditions for the cyclization chemistries, we designed a model peptide that would create a knotted peptide in the theta (θ) conformation[47] when the cyclization chemistries were applied (Figure 1c). We measured the yield and fidelity of incorporation of AzHA and F-yne within a PURE translation lacking methionine and phenylalanine (Figure 1d–h); both were incorporated with good fidelity and yield individually. Incorporation of both amino acids led to a slightly diminished yield and fidelity (Figure 1d and 1e),.

Creation of bicyclic peptides using orthogonal chemistries

We next worked to ensure that we could perform both CuAAC and cysteine-bisalkylation on this model peptide. We reasoned that performing the mild cysteine-bisalkylation first would allow for complete conversion to the monocyclic peptide and minimize any potential decrease in yield and/or fidelity from oxidative by-products generated during the click reaction.[48, 55] We reacted the model peptide with α,α′-dibromo-*m*-xylene and observed complete conversion to the bisthioether benzene-bridged macrocyclic peptide via MALDI-TOF (Supporting Figure S2). The generation of triazole-linked cyclic peptides does not result in a mass change; therefore, we employed 'clickable' external reagents to optimize our click conditions. We prepared a version of our peptide containing only F-yne. When we titrated this peptide with an azide-functionalized sulforhodamine 101 (Texas Red-azide, Figure 2a), we observed concentration-dependent labeling in the presence of click reagents (Figure 2b). Similarly, an AzHA-labeled peptide could be successfully reacted with hex-5-yne-oic acid (Supporting Figure S3a). We then prepared a peptide containing both the AzHA and F-yne. When this peptide was treated with CuAAC reagents prior to addition of 250 μM Texas Red Azide, very little labeling occurred (Figure 2b, lane 9). Similarly, we observed no labeling when hex-5-yne-oic acid was added to the 'pre-clicked' peptide (Supporting Figure S3b). These data, taken together, demonstrate that we can perform both CuAAC and dibromoxylene cyclizations on *in vitro* translated peptides, resulting in the creation of bicyclic peptides.

Compatibility of mRNA display with click chemistry

To create mRNA-displayed peptide libraries, it also is essential that the proposed chemistries do not degrade mRNA. The dibromoxylene cyclization chemistry has already been shown to be compatible with mRNA display.[56, 57, 58] However, others have shown that CuAAC reagents degrade nucleic acids over time and that RNA is particularly susceptible to oxidation.[59, 60] The use of polytriazole ligands, such as tris[(1-benzyl-1H-1,2,3-triazol-4-yl)methyl]amine (TBTA) or the water-soluble tris(3-hydroxypropyl-triazolylmethyl)amine (THPTA), have been shown to protect Cu(I) from oxidation or disproportionation.[61, 62, 63] We tested the compatibility of library mRNA with each ligand and found that mRNA was highly stable up to 2h using click reagents in the presence of TBTA with 33% DMSO relative to the water soluble THPTA (Supporting Figure S4).

Finally, we verified that these optimized click conditions can be applied to an mRNA-peptide fusion library (Figure 3). We first generated mRNA-displayed peptides using our

mixed scaffold libraries designed for selection (Figure 4 and Supporting Table S1), which encode AzHA, F-yne and two cysteines by *in vitro* translation initiated with mRNA covalently linked to puromycin via a poly-A containing linker.[45] The mRNA-peptide fusions were first cyclized by cysteine-bisalkylation while immobilized on oligo(dT) magnetic beads,[58] eluted, and subsequently bound to Ni-NTA resin. We then added 250 μM Texas Red-azide, along with the optimized click reagents, and analyzed the reaction over time by SDS-PAGE. Labeling of the mRNA-peptide fusion library without degradation occurred after 2 h under inert atmosphere (Figure 3). Lastly, we ensured that azide-containing mRNA-peptide fusions were not compromised during the most reductive step in the mRNA display process, reverse transcription, which requires 5 mM DTT and elevated temperatures for 30 min. (Supporting Figure S5). Taken together these experiments show that mRNA displayed peptide libraries are compatible with CuAAC chemistry.

Comparative scaffold-diverse *in vitro* selections

To assess the relative fitness of the bicyclic peptide library generation technology in an mRNA display selection, we chose to perform a side-by-side *in vitro* selection with a monocyclic bisalkylation-based library similar to those we generated previously.[56, 57] We designed five libraries, each containing two cysteine codons (one fixed at the 3′ end of the random region and one that was varied), and one Phe codon that was varied in position between libraries (Figure 4a–c and Supporting Figure S6). The initiator Met codon fixed the position of the azide to the N-terminus. This design resulted in the generation of five libraries which, when cyclized solely with dibromoxylene, resulted in macrocycles with 7–11 amino acids in the rings. However, when subsequently cyclized a second time with CuAAC, these libraries generate highly-constrained, overlapping, θ-bridged scaffolds (Figure 4d).

In vitro selection

As the target for our selection we chose streptavidin, a highly studied protein with a well-defined binding pocket which has been shown in previous selections to prefer constrained peptides.[8, 10, 64] For Round 1 of the parallel selections, we initiated a single translation with an equimolar mix of the five library mRNAs pre-linked to the puromycin oligo; we used incorporation of ^{35}S-cysteine for quantification. While immobilized on oligo(dT) resin, the mRNA-peptide fusion pool was bis-alkylated with α,α′-dibromo-*m*-xylene (Figure 5). At this point, the fusions were split into monocyclic and bicyclic pools, reverse transcribed and captured onto Ni-NTA agarose. The bicyclic pool was clicked to generate the second triazole-containing cycle. The purified monocyclic and bicyclic fusions were independently incubated for 4h with magnetic streptavidin beads. Bound fusions were competitively eluted with D-biotin and separately PCR-amplified to initiate round 2. Stringency was increased by using additional washes of the beads beginning in round 2. While we noted enrichment beginning in round 4 and continuing through round 7 for the monocyclic selection (Supporting Figure S7), we observed no global enrichment throughout the bicyclic selection, despite two additional rounds. The purified PCR-amplified DNA from both selections was then sequenced using the Illumina MiSeq platform.

Sequence analysis

The raw sequencing data was analyzed using AptaTOOLS, a comprehensive software collection designed specifically for the *in silico* processing of several types of *in vitro* selections (Supporting Tables S3 and S4). First, the data was preprocessed using AptaPLEX[65] by filtering out low quality reads and extracting the relevant sequence region. Remaining sequences in each selection cycle were then computationally analyzed using AptaCLUSTER[66] by elucidating and tracking the behavior of aptamers and aptamer families (clusters) throughout the sequenced portion of the selections. In conjunction with its graphical user interface AptaGUI,[67] the algorithm also determined global properties of the selections such as the convergence of the pool towards certain families of sequences, as well as local characteristics including, but not limited to, the abundance and enrichment rate of each individual sequence and cluster respectively. As expected based on the selection enrichment measurement (Supporting Figure S7), the monocyclic selection showed a high level of sequence convergence after 6 rounds (Figure 6a and Supporting Tables S5a and S5b). Moreover, there was a clear scaffold preference—all of the most abundant sequences came from the MXXXXCFXXXXC library. Surprisingly, 4 of the top 8 sequences from the bicyclic selection were also abundant in the monocyclic selection (9.1b=7.1m, 9.2b=7.2m, 9.3b=7.3m, and 9.8b=7.4m), although the percentage of these peptides in the final pool was significantly less (1–2% vs. 20–26%) (Figure 6b and Supporting Tables S6a and S6b). The bicyclic selection also contained peptides that were not found at all in monocyclic selection winners (9.4b and 9.6b) as well as a linear mutant which did not contain a F-yne or a second cysteine (9.5lin). Based on these results, we decided to further analyze peptides 7.1m–7.4m in the linear, mono- and bicyclic configurations as well as peptide 9.4b, which was the most abundant, unique bicyclic peptide. Finally, we also analyzed linear peptide 9.5lin as a point of comparison.

Affinity for streptavidin

Each of the peptides was prepared with *in vitro* translation in the presence of ^{35}S-Cys, and the pertinent cyclization steps were carried out while the peptide was immobilized on Ni-NTA resin. The purity of the peptides was verified by MALDI-TOF (Supporting Figure S8). As an initial screen for affinity, we chose to test each peptide in its linear, mono-, and bicyclic forms for its ability to bind to 1 μM immobilized streptavidin. The four most abundant monocyclic selection winners (7.1m–7.4m) all showed enhanced binding to streptavidin in their monocyclic conformations relative to the linear and bicyclic forms (Figure 7a). The unique 9.4b bicyclic peptide showed binding in both the monocyclic and bicyclic configurations, although the bicyclic configuration bound to the greatest extent. Since this peptide contained two F-yne residues (Figure 7b), there are two potential places for the click cyclization to occur. To test the preference, we independently substituted each of the F-yne residues with tyrosine giving 9.4b-7Y and 9.4b-10Y, to force the triazole-containing ring sizes to 10 or 7 amino acid-sized rings respectively. The knotted peptide containing the 10AA triazole cycle (9.4b-7Y) bound to a much greater extent than the 7AA ring (Figure 8b). We next determined the absolute affinity of our top binding *in vitro* translated peptides (7.2m, 7.3m, 9.4b, and 9.4b7Y) using a magnetic bead-based version of the spin filter binding-inhibition assay[68] (Figure 7c, Supporting Figure S9 and S10). Both

7.2m and 7.3m had K_ds of approximately 300–400 nM. 9.4b as well as the 9.4b7Y mutant had K_ds in the 500–600 nM range.

The second cyclization enhances protease stability

Others have demonstrated that cyclic and knotted peptides from libraries are far more biostable and remarkably resistant to enzymatic degradation,[26, 69] qualities that increase their therapeutic potential. To compare, we selected the linear (9.5lin), monocyclic (7.2m) and bicyclic peptide (9.4b) variants and incubated them with immobilized chymotrypsin. At each time point, we removed an aliquot of peptide and measured its ability to bind immobilized streptavidin. As expected, the binding activity of the linear peptide was almost completely abolished after 1h. The monocyclic peptide 7.2m displayed greater resistance to protease degradation, retaining 57% of its binding activity after 24h relative to the control (Figure 8). Interestingly, and in accordance with our hypothesis, 96% of bicyclic peptide 9.4b was able to bind to streptavidin after 24h incubation with chymotrypsin. Furthermore, even after extended incubation with the protease, the bicyclic peptide showed remarkable retention of binding activity, despite the fact that it had an additional predicted cleavage site relative to the monocyclic peptide (Supporting Figure S11).

The advent of Next Generation Sequencing (NGS) has proven to be a powerful tool in the ligand discovery/DNA template-based selection field.[70] When combined with software such as AptaTools, which allows in-depth round-by-round analysis of enrichment rates, important ligands which may have otherwise gone unnoticed can now be uncovered. For the monocyclic selection, we observed high enrichment rates from round 4 to round 5 while the subsequent increase in the remaining rounds for each of the monocyclic peptides was much more moderate. This pairs nicely with our selection enrichment results based on radioactivity (Supporting Figure S7) and suggests that the selection had plateaued after round 5. At round 5 however, the abundance of the winner sequences was still quite low (<4%)--too low to meaningfully detect these sequences by traditional Sanger sequencing. Therefore, in principle, use of NGS and Aptatools could shorten the number of rounds necessary to detect winners as compared to standard sequencing. For the bicyclic selection, we did not see detectable global enrichment (Supporting Figure S7), yet after analysis by NGS, certain individual sequences were enriched. Because they were still at low abundance at the end of the selection, the use of NGS was essential for the identification of peptide 9.4b as a streptavidin binder.

Our monocyclic streptavidin binding-peptides have unique sequence motifs as compared to previous selections. For example, the HPQ motif revealed in numerous selections against streptavidin[10, 71, 72, 73] was absent from our most abundant sequences in the monocyclic selection. Instead, sequencing revealed a consensus binding motif that included portions of the N-terminal linear and C-terminal cyclic regions (Supporting Figure S12). The only significant variability in the top 8 monocyclic sequences was in the final randomized position. The fact that these peptides showed much weaker affinity in their linear forms leads us to conclude that cyclization of these sequences is essential for a high affinity interaction with streptavidin. When we added a second cycle to these peptides, the binding

was dramatically reduced (Figure 7a). This is to be expected, because the second cycle will dramatically change the conformation of these peptides (Figure 4d).

Peptide 9.4b derived from the bicyclic selection, in contrast, did bind effectively in its bicyclic form. This peptide has two F-yne residues as potential cyclization points. When we removed each of these in turn, only the bicyclic peptide with the F-yne at position 10 led to effective binding (Figure 7b). This is significant, because this F-yne was located in the random region of the library, while the F-yne at position 7 was fixed. From a library design standpoint, this is quite interesting; this peptide effectively "chose" a scaffold that was underrepresented in the library. Our low enrichment rates from the bicyclic selection could, therefore, be a consequence of our biased scaffold choice.

The peptide winners common to the two selections (Figure 6a,b) did not bind to streptavidin in their bicyclic configurations (Figure 7a). It is therefore quite surprising that these sequences were present in the bicyclic selection winners. First, we note that the enrichment rates of these peptides are quite low in comparison to the enrichment values in the monocyclic selection prior to its plateau. The low global enrichment explains why we did not see significant convergence in sequences, even though we performed 2 additional rounds relative to the monocyclic selection. While we demonstrated that the click cyclization results in high conversion to the bicyclic peptide using our model peptide (Supporting Figures S2 and S3a,b), it is certainly possible that the cyclization efficiencies of these sequences under selection conditions are less than 100%. If so, the low global enrichment could be due to the presence of the monocyclic sequences during the bicyclic selection. Also, although we were very careful to avoid this, we cannot definitively rule out that cross contamination could be responsible for the presence of the monocyclic sequences in the bicyclic library since the selections were performed side-by-side.

In summary, we have developed a technology to create highly-constrained bicyclic peptides *in situ* using a cell-free translation system, and we have optimized the method to make it compatible with mRNA display to generate mRNA-bicyclic peptide fusions for *in vitro* selection. We designed our parallel selection strategy in order to evaluate the potential for the mono- and bicyclic libraries to uncover peptide binders. We conclude that high-affinity versions of both types of ligands are present in the diverse libraries we created; however, the bicyclic peptides have the advantage of dramatically enhanced protease stability. Moreover, because we have fixed the position of the cyclization residues to only a few possibilities, we have only probed a very small subset of the potential diversity of these bicyclic libraries. It should therefore now be possible to randomize these positions to create a whole host of highly-constrained peptide libraries using mRNA display. We believe that the high level of scaffold diversity generated using this strategy should enable the discovery of protease-stable bicyclic ligands to not only targets already probed by bicyclic peptides (e.g. kallikrein[38] and human urokinase-type plasminogen activator[18, 39]) but also many therapeutic targets that do not currently have potent inhibitors.

Methods

mRNA stability with click reagents (TBTA vs. THPTA)

CuAAC reagents (100 mM potassium phosphate pH 8, 500 mM NaCl, 1 mM $CuSO_4$) were added to two 0.6mL microcentrifuge tubes along with 5 μM mRNA (202 bases). Tube 1 contained 2 mM TBTA ligand w/33% (v/v) DMSO; Tube 2, 10 mM THPTA ligand. Tubes were degassed with argon, 10 mM sodium ascorbate was added and a small septum was used to seal each tube. A blanket of argon was placed over each reaction mixture. Total volume of each tube was 100 μL. At the indicated time points, 20 μL was removed from each tube with a microsyringe, quenched with 5 μL of 200 mM EDTA and frozen at −20°C. Time points were analyzed by 10% urea-PAGE, stained with ethidium bromide and imaged on a ChemiDoc MP imaging system (BioRad).

Preparation of mRNA-peptide fusion library

T7 *in vitro* transcription[74] was performed with an equimolar mix of the five bottom strand oligo libraries (see Table S1), following pre-annealing to the forward primer (70° C for 5min, followed by cooling on ice for 1min.). Library mRNA was photo-crosslinked to the linker containing puromycin at the 3′end as described previously.[75] For round 1 of the parallel selections, a single 2 mL standard translation reaction was initiated with the addition of the puromyocin-linked mRNA, incubated at 37° C for 1.25 h, supplemented with 550 mM KCl and 55 mM $MgCl_2$, returned to the incubator for 1.5h and subsequently frozen overnight at −80° C. The resulting mRNA-peptide fusions were diluted 6-fold with oligo-dT binding buffer (20 mM Tris-HCl pH 7.8, 10 mM EDTA, 1 M NaCl, 0.2% Triton X-100, 0.5 mM TCEP), added to 1.5 mL of oligo-dT magnetic beads which were equilibrated thrice with 5 mL of oligo-dT binding buffer, and rotated at 4° C for 30 min. The beads were washed twice with 5 mL of oligo-dT wash buffer (20 mM Tris-HCl pH 7.8, 0.3 M NaCl, 0.1% Triton X-100, 0.5 mM TCEP), and the first cyclization was performed on resin by the addition of 5 mL of cyclization buffer (20 mM Tris-HCl pH 7.8, 0.66 M NaCl, 3 mM α,α′-dibromo-*m*-xylene, 33% acetonitrile (v/v), 0.5 mM TCEP) and rotated at RT for 30 min. The beads were washed once with 5 mL of oligo-dT wash buffer containing 5 mM BME (in lieu of TCEP), to quench the unreacted linker. Beads were washed a second time with 5 mL of wash buffer containing TCEP and eluted in 1 mL fractions with 0.5 mM TCEP. The five elutions with the highest scintillation counts were pooled and precipitated with 4 vol of ethanol, 0.1 vol of 3 M KOAc, pH 5.2 and 0.001 vol of 5 mg/mL glycogen. The pellet was resuspended in 543.5 μL of water and split into two portions for the monocyclic and bicyclic selections.

Monocyclic—One half of this solution was reverse transcribed in a final volume of 400 μL in the presence of RT mix (0.5 μM RT primer, 0.5 mM dNTPs, 5 mM $MgCl_2$, 1 mM DTT, 2 U/μL RNase inhibitor, 5 U/μL Superscript III, 1× First Strand buffer) at 55° C for 30 min. The RT reactions were subsequently diluted 5-fold with denaturing Ni-NTA binding buffer (100 mM NaH_2PO_4, 10 mM Tris-HCl, 6 M guanidinium hydrochloride, 0.2% Triton X-100, 5 mM BME, pH 8) and added to 100 μL of Ni-NTA agarose resin (MCLab) in a 10 mL BioRad disposable column. Columns were placed on a tumbler at 4° C for 1h. The monocyclic fusions were washed four times with 3 mL of Ni-NTA wash buffer (100 mM

NaH_2PO_4, 300 mM NaCl, 0.2% Triton X-100, 5 mM BME, pH 8) and eluted in one column volume fractions with Ni-NTA elution buffer (50 mM NaH_2PO_4, 300 mM NaCl, 350 mM imidazole, 0.2% Triton X-100, 5 mM BME, pH 8). Fractions containing significant radioactivity were pooled and dialyzed overnight against selection buffer (50 mM Tris-HCl pH 8, 150 mM NaCl, 4 mM $MgCl_2$, 0.25% Triton X-100).

Bicyclic—The second half of this solution was reverse transcribed in a final volume of 400 μL in the presence of RT mix (0.5 μM RT primer, 0.5 mM dNTPs, 5 mM $MgCl_2$, 1 mM DTT, 2 U/μL RNase inhibitor, 5 U/μL Superscript III, 1× First Strand buffer) at 55° C for 30 min. The RT reactions were subsequently diluted 5-fold with denaturing Ni-NTA binding buffer (100 mM NaH_2PO_4, 10 mM Tris-HCl, 6 M guanidinium hydrochloride, 0.2% Triton X-100, 5 mM BME, pH 8) and added to 100 μL of Ni-NTA agarose resin (MCLab) in a 10 mL BioRad disposable column. Columns were placed on a tumbler at 4° C for 1h. After binding to the Ni-NTA agarose, bicyclic fusions were washed once with 3 mL of Ni-NTA wash buffer, and 3 mL total volume of CuAAC cyclization reagents were added (100mM phosphate pH 8, 1 mM $CuSO_4$, 300 mM NaCl, 2 mM TBTA, 33% DMSO (v/v). The solution was degassed with argon prior to the addition of 10 mM sodium ascorbate. An argon blanket was placed over the solution, the tube was sealed and rotated at room temperature for 2h. After incubation, the resin was washed once with 3 mL of Ni-NTA wash buffer containing 10% DMSO (v/v). Following two additional washes with 3 mL of Ni-NTA wash buffer, the purified fusions were eluted, pooled and dialyzed similarly to the monocyclic fusions.

The translation volume was reduced to 500 μL for rounds 2–4, 250 μL for rounds 5–7. Purification reagent usage, wash and elution volumes were adjusted accordingly to coincide with translation yield.

Selection against streptavidin

Two tubes containing 125 μL Dynabeads M-280 Streptavidin (Invitrogen #11205D) were equilibrated twice with 1 mL selection buffer and 0.5 pmols (3.01×10^{11} fusions, 11.75-fold above theoretical library diversity) each of monocyclic or bicyclic dialyzed fusions (125 μL total volume) were added to the respective tubes (with 0.1% BSA) and rotated at 4° C for 1h. The beads were then washed twice with 1 mL selection buffer and streptavidin-binding fusions were competitively eluted for 4h (to account for slow off-rates) with 200 μL of 2 mM D-biotin in selection buffer. Eluted fusions (2.4% and 2.0% of monocyclic and bicyclic input, respectively) were dialyzed overnight against 0.1% Triton X-100. Following PCR amplification using ExtT7fwd and UniRev2 primers (2 min. at 94°C, followed by 24 rounds of 94° C (30s), 65° C (30s), 72° C (45s), library DNA was extracted with 1 volume of phenol:chloroform:isoamyl alcohol (25:24:1) and precipitated with 3 vol. ethanol and 0.1 vol 3 M KOAc pH 5.2. The resuspended DNA served as the templates for Round 2 of the parallel selections. The bead-to-fusion volume ratio was kept constant throughout the selection.

Relative streptavidin binding

In vitro transcribed and radiolabeled peptides prepared as described in the Supporting Information were diluted in SBB to 20 nM. 10 μL of M-280 streptavidin beads were equilibrated three times each with 100 μL of SBB. The beads were bound to a magnetic stand, the buffer was removed and 20 μL was added to each tube. The beads were resuspended with diluted peptide solution, resulting in approximate streptavidin-on-bead concentration of 1 μM, calculated based on manufacturer's reported biotin binding capacity. Tubes were placed on a rotisserie at 4° C for 2h, then placed on the magnetic stand and the supernatant was removed. The beads were washed twice each with four CV of SBB (with mild vortex to ensure resuspension). Washes were combined with the flow through and a portion was counted via scintillation and considered as the unbound fraction. 200 μL of SBB with 2.5 mM D-biotin was added to each tube and rotated at RT for 2h. The supernatant was removed and a portion was counted as the bound fraction. Fractional, or % bound to streptavidin and eluted with D-biotin, was calculated with the following equation: % bound = [bound/(unbound + bound) × 100]. % bound was determined for each peptide and the highest relative binders for each of the three conformations were selected for further study.

Determination of peptide K_d

In vitro translated, radiolabeled peptides prepared as described above were diluted in SBB to 8 nM and added 1:3 to streptavidin in SBB (1.2 nM – 20 μM final 4-fold serial dilution), resulting in 2 nM peptide final concentration in 20 μL total volume. Reactions were incubated at 4° C for 2h and added to 10 μL washed and dried Dynabeads M-280 streptavidin magnetic beads, mixed and incubated for 1 min at RT. Tubes were then placed on a magnetic stand for 1 min and the supernatant was removed. 17 μL of the supernatant was added to 2 mL of Econo-Safe scintillation fluid (RPI) and counted on a Beckman scintillation counter for 5 min. This was the fraction which bound the free streptavidin (B). The beads were resuspended in 50 uL of SBB, vortexed vigorously and 40 uL was counted as above. This was the unbound fraction which was capable of binding the matrix (U). Fractional binding was then calculated using the following equation: % bound = B/(B+U) × 100%. To account for the portion of the affinity purified peptide mixture incapable of binding streptavidin (primarily unincorporated radiolabel which bound the nickel resin), the assay containing no free streptavidin was subtracted from each streptavidin-containing assay, effectively providing a baseline for % bound calculation. Data was then plotted using SigmaPlot and a curve was generated using a hyperbolic dynamic fit with the following equation: $y = y_o + [ax/(b+x)]$. Experiments were done in at least duplicate.

Chymotrypsin stability assay

Linear, monocyclic and bicyclic labeled peptides, prepared as described in the Supporting Information, which showed the highest relative streptavidin affinity were selected for the protease stability experiment. Surface-activated magnetic beads (Dynabeads M-270 epoxy, Invitrogen #14301) were decorated with α-chymotrypsin (Sigma, C4129) per manufacturer's instructions. Peptides were diluted to 8 nM with streptavidin binding buffer (SBB, 40 mM Tris-HCl pH 7.4, 300 mM KCl, 2 mM EDTA, 5 mM BME, 0.013% Triton X-100) and 350 μL (2.8 pmols) of each peptide was added to 1.4 U of chymotrypsin beads

(unit calculation based on chymotrypsin functionalization input and assumes 100% conjugation efficiency and retention of activity) in a 1.7 mL tube and placed on a tumbler at RT. At the indicated time points the tube was placed on a magnetic stand and 25 μL was removed from the tube and placed at −20° C. After 24 h the reaction was incubated for an additional 24 h at 37°C. Each time point was thawed on ice, mixed and 10 μL was added to 5 μL of M-280 streptavidin beads pre-equilibrated three times with 200 μL of SBB. The solution was allowed to reach equilibrium on a rotisserie at 4° C for 2h. Tubes were bound to the magnetic stand and the supernatant removed. The beads were washed twice each with four CV of SBB. The washes were combined with the supernatant, mixed and a portion was counted via scintillation as unbound peptide. 200 μL of SBB containing 2.5 mM D-biotin was added to the beads and tubes were rotated at RT for 2 h to selectively elute the bound labeled peptides. After binding to the magnet, the supernatant was removed, and a portion was counted as bound peptide. Fractional, or % binding to streptavidin was calculated with the following equation: % bound = [bound/(unbound + bound) × 100]. % bound for each peptide was normalized to the no chymotrypsin (0 time) control and plotted as a function of time.

Supplementary Material

Refer to Web version on PubMed Central for supplementary material.

Acknowledgments

The authors would like to thank D. Selaya Hawkins for synthesizing the azide-functionalized sulforhodamine 101 (Texas Red azide) used in the CuAAC validation experiments. We also thank J. Sheldon and S. Richardson for providing scientific insight. The authors acknowledge financial support of this work from the NIH (R01CA166264). The MALDI-TOF instrument is part of the MCC Proteomics Resource supported by CCSG grant NCI 5P30CA16059-35.

References

1. Nguyen LT, Chau JK, Perry NA, De Boer L, Zaat SA, Vogel HJ. Serum stabilities of short tryptophan-and arginine-rich antimicrobial peptide analogs. PLoS One. 2010; 5:e12684. [PubMed: 20844765]
2. Molhoek EM, Van Dijk A, Veldhuizen EJ, Haagsman HP, Bikker FJ. Improved proteolytic stability of chicken cathelicidin-2 derived peptides by D-amino acid substitutions and cyclization. Peptides. 2011; 32:875–880. [PubMed: 21376095]
3. Clark RJ, Fischer H, Dempster L, Daly NL, Rosengren KJ, Nevin ST, Meunier FA, Adams DJ, Craik DJ. Engineering stable peptide toxins by means of backbone cyclization: Stabilization of the alpha-conotoxin MII. Proc Natl Acad Sci U S A. 2005; 102:13767–13772. [PubMed: 16162671]
4. Matsuzaki K. Control of cell selectivity of antimicrobial peptides. Biochim Biophys Acta, Biomembr. 2009; 1788:1687–1692.
5. Rozek A, Powers JS, Friedrich CL, Hancock RE. Structure-based design of an indolicidin peptide analogue with increased protease stability. Biochemistry. 2003; 42:14130–14138. [PubMed: 14640680]
6. Passioura T, Katoh T, Goto Y, Suga H. Selection-based discovery of druglike macrocyclic peptides. Annu Rev Biochem. 2014; 83:727–752. [PubMed: 24580641]
7. Bock JE, Gavenonis J, Kritzer JA. Getting in shape: Controlling peptide bioactivity and bioavailability using conformational constraints. ACS Chem Biol. 2012; 8:488–499. [PubMed: 23170954]

8. Meyer SC, Gaj T, Ghosh I. Highly selective cyclic peptide ligands for NeutrAvidin and avidin identified by phage display. Chem Biol Drug Des. 2006; 68:3–10. [PubMed: 16923020]
9. Katz BA. Binding to protein targets of peptidic leads discovered by phage display: Crystal structures of streptavidin-bound linear and cyclic peptide ligands containing the HPQ sequence. Biochemistry. 1995; 34:15421–15429. [PubMed: 7492542]
10. Giebel LB, Cass R, Milligan DL, Young D, Arze R, Johnson C. Screening of cyclic peptide phage libraries identifies ligands that bind streptavidin with high affinities. Biochemistry. 1995; 34:15430–15435. [PubMed: 7492543]
11. Getz JA, Rice JJ, Daugherty PS. Protease-resistant peptide ligands from a knottin scaffold library. ACS Chem Biol. 2011; 6:837–844. [PubMed: 21615106]
12. Piserchio A, Salinas GD, Li T, Marshall J, Spaller MR, Mierke DF. Targeting specific PDZ domains of PSD-95: Structural basis for enhanced affinity and enzymatic stability of a cyclic peptide. Chem Biol. 2004; 11:469–473. [PubMed: 15123241]
13. DiMaio J, Nguyen TM, Lemieux C, Schiller PW. Synthesis and pharmacological characterization in vitro of cyclic enkephalin analogs: Effect of conformational constraints on opiate receptor selectivity. J Med Chem. 1982; 25:1432–1438. [PubMed: 6296388]
14. Gudmundsson OS, Pauletti GM, Wang W, Shan D, Zhang H, Wang B, Borchardt RT. Coumarinic acid-based cyclic prodrugs of opioid peptides that exhibit metabolic stability to peptidases and excellent cellular permeability. Pharm Res. 1999; 16:7–15. [PubMed: 9950272]
15. Kwon Y, Kodadek T. Quantitative comparison of the relative cell permeability of cyclic and linear peptides. Chem Biol. 2007; 14:671–677. [PubMed: 17584614]
16. Rezai T, Bock JE, Zhou MV, Kalyanaraman C, Lokey RS, Jacobson MP. Conformational flexibility, internal hydrogen bonding, and passive membrane permeability: Successful in silico prediction of the relative permeabilities of cyclic peptides. J Am Chem Soc. 2006; 128:14073–14080. [PubMed: 17061890]
17. Hewitt WM, Leung SS, Pye CR, Ponkey AR, Bednarek M, Jacobson MP, Lokey RS. Cell-permeable cyclic peptides from synthetic libraries inspired by natural products. J Am Chem Soc. 2015; 137:715–721. [PubMed: 25517352]
18. Angelini A, Cendron L, Chen S, Touati J, Winter G, Zanotti G, Heinis C. Bicyclic peptide inhibitor reveals large contact interface with a protease target. ACS Chem Biol. 2012; 7:817–821. [PubMed: 22304751]
19. Bionda N, Fasan R. Ribosomal synthesis of Natural-Product-Like bicyclic peptides in escherichia coli. ChemBioChem. 2015; 16:2011–2016. [PubMed: 26179106]
20. Bartoloni M, Jin X, Marcaida MJ, Banha J, Dibonaventura I, Bongoni S, Bartho K, Gräbner O, Sefkow M, Darbre T. Bridged bicyclic peptides as potential drug scaffolds. Chem Sci. 2015; 6:5473–5490.
21. Lian W, Jiang B, Qian Z, Pei D. Cell-permeable bicyclic peptide inhibitors against intracellular proteins. J Am Chem Soc. 2014; 136:9830–9833. [PubMed: 24972263]
22. Trinh TB, Upadhyaya P, Qian Z, Pei D. Discovery of a direct ras inhibitor by screening a combinatorial library of cell-permeable bicyclic peptides. ACS Comb Sci. 2015; 18:75–85. [PubMed: 26645887]
23. Quartararo JS, Eshelman MR, Peraro L, Yu H, Baleja JD, Lin Y, Kritzer JA. A bicyclic peptide scaffold promotes phosphotyrosine mimicry and cellular uptake. Bioorg Med Chem. 2014; 22:6387–6391. [PubMed: 25438762]
24. Wang CK, Hu SH, Martin JL, Sjogren T, Hajdu J, Bohlin L, Claeson P, Goransson U, Rosengren KJ, Tang J, Tan NH, Craik DJ. Combined X-ray and NMR analysis of the stability of the cyclotide cystine knot fold that underpins its insecticidal activity and potential use as a drug scaffold. J Biol Chem. 2009; 284:10672–10683. [PubMed: 19211551]
25. Saez NJ, Senff S, Jensen JE, Er SY, Herzig V, Rash LD, King GF. Spider-venom peptides as therapeutics. Toxins. 2010; 2:2851–2871. [PubMed: 22069579]
26. Colgrave ML, Craik DJ. Thermal, chemical, and enzymatic stability of the cyclotide kalata B1: The importance of the cyclic cystine knot. Biochemistry. 2004; 43:5965–5975. [PubMed: 15147180]

27. Tam JP, Lu YA, Yang JL, Chiu KW. An unusual structural motif of antimicrobial peptides containing end-to-end macrocycle and cystine-knot disulfides. Proc Natl Acad Sci U S A. 1999; 96:8913–8918. [PubMed: 10430870]
28. Tang YQ, Yuan J, Osapay G, Osapay K, Tran D, Miller CJ, Ouellette AJ, Selsted ME. A cyclic antimicrobial peptide produced in primate leukocytes by the ligation of two truncated alpha-defensins. Science. 1999; 286:498–502. [PubMed: 10521339]
29. Kim J, Park S, Hwang I, Cheong H, Nah J, Hahm K, Park Y. Protease inhibitors from plants with antimicrobial activity. Int J Mol Sci. 2009; 10:2860–2872. [PubMed: 19582234]
30. Le Nguyen D, Heitz A, Chiche L, Castro B, Boigegrain R, Favel A, Coletti-Previero M. Molecular recognition between serine proteases and new bioactive microproteins with a knotted structure. Biochimie. 1990; 72:431–435. [PubMed: 2124146]
31. Daly NL, Ekberg JA, Thomas L, Adams DJ, Lewis RJ, Craik DJ. Structures of muO-conotoxins from conus marmoreus. I nhibitors of tetrodotoxin (TTX)-sensitive and TTX-resistant sodium channels in mammalian sensory neurons. J Biol Chem. 2004; 279:25774–25782. [PubMed: 15044438]
32. Olivera BM, Rivier J, Clark C, Ramilo CA, Corpuz GP, Abogadie FC, Mena EE, Woodward SR, Hillyard DR, Cruz LJ. Diversity of conus neuropeptides. Science. 1990; 249:257–263. [PubMed: 2165278]
33. Olivera BM. Conus peptides: Biodiversity-based discovery and exogenomics. J Biol Chem. 2006; 281:31173–31177. [PubMed: 16905531]
34. Moore SJ, Hayden Gephart MG, Bergen JM, Su YS, Rayburn H, Scott MP, Cochran JR. Engineered knottin peptide enables noninvasive optical imaging of intracranial medulloblastoma. Proc Natl Acad Sci U S A. 2013; 110:14598–14603. [PubMed: 23950221]
35. Kimura RH, Teed R, Hackel BJ, Pysz MA, Chuang CZ, Sathirachinda A, Willmann JK, Gambhir SS. Pharmacokinetically stabilized cystine knot peptides that bind alpha-v-beta-6 integrin with single-digit nanomolar affinities for detection of pancreatic cancer. Clin Cancer Res. 2012; 18:839–849. [PubMed: 22173551]
36. Cox N, Kintzing JR, Smith M, Grant GA, Cochran JR. Integrin-Targeting knottin Peptide–Drug conjugates are potent inhibitors of tumor cell proliferation. Angew Chem, Int Ed. 2016; 55:9894–9897.
37. Timmerman P, Beld J, Puijk WC, Meloen RH. Rapid and quantitative cyclization of multiple peptide loops onto synthetic scaffolds for structural mimicry of protein surfaces. ChemBioChem. 2005; 6:821–824. [PubMed: 15812852]
38. Baeriswyl V, Rapley H, Pollaro L, Stace C, Teufel D, Walker E, Chen S, Winter G, Tite J, Heinis C. Bicyclic peptides with optimized ring size inhibit human plasma kallikrein and its orthologues while sparing paralogous proteases. ChemMedChem. 2012; 7:1173–1176. [PubMed: 22492508]
39. Heinis C, Rutherford T, Freund S, Winter G. Phage-encoded combinatorial chemical libraries based on bicyclic peptides. Nat Chem Biol. 2009; 5:502–507. [PubMed: 19483697]
40. Chen S, Bertoldo D, Angelini A, Pojer F, Heinis C. Peptide ligands stabilized by small molecules. Angew Chem, Int Ed. 2014; 53:1602–1606.
41. Chen S, Rentero Rebollo I, Buth SA, Morales-Sanfrutos J, Touati J, Leiman PG, Heinis C. Bicyclic peptide ligands pulled out of cysteine-rich peptide libraries. J Am Chem Soc. 2013; 135:6562–6569. [PubMed: 23560397]
42. Rentero Rebollo I, Sabisz M, Baeriswyl V, Heinis C. Identification of target-binding peptide motifs by high-throughput sequencing of phage-selected peptides. Nucleic Acids Res. 2014; 42:e169. [PubMed: 25348396]
43. Feener EP, Shen WC, Ryser HJ. Cleavage of disulfide bonds in endocytosed macromolecules. A processing not associated with lysosomes or endosomes. J Biol Chem. 1990; 265:18780–18785. [PubMed: 2229041]
44. Yang J, Chen H, Vlahov IR, Cheng JX, Low PS. Evaluation of disulfide reduction during receptor-mediated endocytosis by using FRET imaging. Proc Natl Acad Sci U S A. 2006; 103:13872–13877. [PubMed: 16950881]
45. Roberts RW, Szostak JW. RNA-peptide fusions for the in vitro selection of peptides and proteins. Proc Natl Acad Sci U S A. 1997; 94:12297–12302. [PubMed: 9356443]

46. Nemoto N, Miyamoto-Sato E, Husimi Y, Yanagawa H. In vitro virus: Bonding of mRNA bearing puromycin at the 3′-terminal end to the C-terminal end of its encoded protein on the ribosome in vitro. FEBS Lett. 1997; 414:405–408. [PubMed: 9315729]
47. Tezuka Y, Oike H. Topological polymer chemistry: Systematic classification of nonlinear polymer topologies. J Am Chem Soc. 2001; 123:11570–11576. [PubMed: 11716710]
48. Kolb HC, Finn M, Sharpless KB. Click chemistry: Diverse chemical function from a few good reactions. Angew Chem, Int Ed. 2001; 40:2004–2021.
49. Sako Y, Morimoto J, Murakami H, Suga H. Ribosomal synthesis of bicyclic peptides via two orthogonal inter-side-chain reactions. J Am Chem Soc. 2008; 130:7232–7234. [PubMed: 18479111]
50. Josephson K, Hartman MC, Szostak JW. Ribosomal synthesis of unnatural peptides. J Am Chem Soc. 2005; 127:11727–11735. [PubMed: 16104750]
51. Kirshenbaum K, Carrico IS, Tirrell DA. Biosynthesis of proteins incorporating a versatile set of phenylalanine analogues. ChemBioChem. 2002; 3:235–237. [PubMed: 11921403]
52. Link AJ, Vink MK, Agard NJ, Prescher JA, Bertozzi CR, Tirrell DA. Discovery of aminoacyl-tRNA synthetase activity through cell-surface display of noncanonical amino acids. Proc Natl Acad Sci U S A. 2006; 103:10180–10185. [PubMed: 16801548]
53. Kiick KL, Saxon E, Tirrell DA, Bertozzi CR. Incorporation of azides into recombinant proteins for chemoselective modification by the staudinger ligation. Proc Natl Acad Sci U S A. 2002; 99:19–24. [PubMed: 11752401]
54. Hartman MC, Josephson K, Lin CW, Szostak JW. An expanded set of amino acid analogs for the ribosomal translation of unnatural peptides. PLoS One. 2007; 2:e972. [PubMed: 17912351]
55. Hong V, Presolski SI, Ma C, Finn M. Analysis and optimization of Copper-Catalyzed Azide–Alkyne cycloaddition for bioconjugation. Angew Chem, Int Ed. 2009; 48:9879–9883.
56. White ER, Sun L, Ma Z, Beckta JM, Danzig BA, Hacker DE, Huie M, Williams DC, Edwards RA, Valerie K. Peptide library approach to uncover phosphomimetic inhibitors of the BRCA1 C-terminal domain. ACS Chem Biol. 2015; 10:1198–1208. [PubMed: 25654734]
57. Guillen Schlippe YV, Hartman MC, Josephson K, Szostak JW. In vitro selection of highly modified cyclic peptides that act as tight binding inhibitors. J Am Chem Soc. 2012; 134:10469–10477. [PubMed: 22428867]
58. Ma Z, Hartman MC. In vitro selection of unnatural cyclic peptide libraries via mRNA display. Ribosome Display and Related Technologies: Methods and Protocols. 2012:367–390.
59. Paredes E, Das SR. Click chemistry for rapid labeling and ligation of RNA. ChemBioChem. 2011; 12:125–131. [PubMed: 21132831]
60. Abel GR Jr, Calabrese ZA, Ayco J, Hein JE, Ye T. Measuring and suppressing the oxidative damage to DNA during cu (I)-catalyzed Azide–Alkyne cycloaddition. Bioconjugate Chem. 2016; 27:698–704.
61. Chen X, Khairallah GN, Richard A, Williams SJ. Fixed-charge labels for simplified reaction analysis: 5-hydroxy-1, 2, 3-triazoles as byproducts of a copper (I)-catalyzed click reaction. Tetrahedron Lett. 2011; 52:2750–2753.
62. Hong V, Steinmetz NF, Manchester M, Finn M. Labeling live cells by copper-catalyzed alkyne–azide click chemistry. Bioconjugate Chem. 2010; 21:1912–1916.
63. Kennedy DC, McKay CS, Legault MC, Danielson DC, Blake JA, Pegoraro AF, Stolow A, Mester Z, Pezacki JP. Cellular consequences of copper complexes used to catalyze bioorthogonal click reactions. J Am Chem Soc. 2011; 133:17993–18001. [PubMed: 21970470]
64. Mendes K, Ndungu JM, Clark LF, Kodadek T. Optimization of the magnetic recovery of hits from one-bead–one-compound library screens. ACS Comb Sci. 2015; 17:506–517. [PubMed: 26221913]
65. Hoinka J, Przytycka T. AptaPLEX–A dedicated, multithreaded demultiplexer for HT-SELEX data. Methods. 2016; 106:82–85. [PubMed: 27080809]
66. Hoinka J, Berezhnoy A, Dao P, Sauna ZE, Gilboa E, Przytycka TM. Large scale analysis of the mutational landscape in HT-SELEX improves aptamer discovery. Nucleic Acids Res. 2015; 43:5699–5707. [PubMed: 25870409]

67. Hoinka J, Dao P, Przytycka TM. AptaGUI-A graphical user interface for the efficient analysis of HT-SELEX data. Mol Ther --Nucleic Acids. 2015; 4:e257. [PubMed: 26461977]

68. Keefe AD, Wilson DS, Seelig B, Szostak JW. One-step purification of recombinant proteins using a nanomolar-affinity streptavidin-binding peptide, the SBP-tag. Protein Expression Purif. 2001; 23:440–446.

69. Garcia EA, Camarero AJ. Biological activities of natural and engineered cyclotides, a novel molecular scaffold for peptide-based therapeutics. Curr Mol Pharmacol. 2010; 3:153–163. [PubMed: 20858197]

70. Jalali-Yazdi F, Huong Lai L, Takahashi TT, Roberts RW. High-Throughput measurement of binding kinetics by mRNA display and Next-Generation sequencing. Angew Chem. 2016; 128:4075–4078.

71. Devlin JJ, Panganiban LC, Devlin PE. Random peptide libraries: A source of specific protein binding molecules. Science. 1990; 249:404–406. [PubMed: 2143033]

72. Gissel B, Jensen MR, Gregorius K, Elsner HI, Svendsen I, Mouritsen S. Identification of avidin and streptavidin binding motifs among peptides selected from a synthetic peptide library consisting solely of d-amino acids. J Pept Sci. 1995; 1:217–226. [PubMed: 9222999]

73. Wilson DS, Keefe AD, Szostak JW. The use of mRNA display to select high-affinity protein-binding peptides. Proc Natl Acad Sci U S A. 2001; 98:3750–3755. [PubMed: 11274392]

74. Milligan JF, Uhlenbeck OC. [5] synthesis of small RNAs using T7 RNA polymerase. Methods Enzymol. 1989; 180:51–62. [PubMed: 2482430]

75. Kurz M, Gu K, Lohse PA. Psoralen photo-crosslinked mRNA-puromycin conjugates: A novel template for the rapid and facile preparation of mRNA-protein fusions. Nucleic Acids Res. 2000; 28:E83. [PubMed: 10982894]

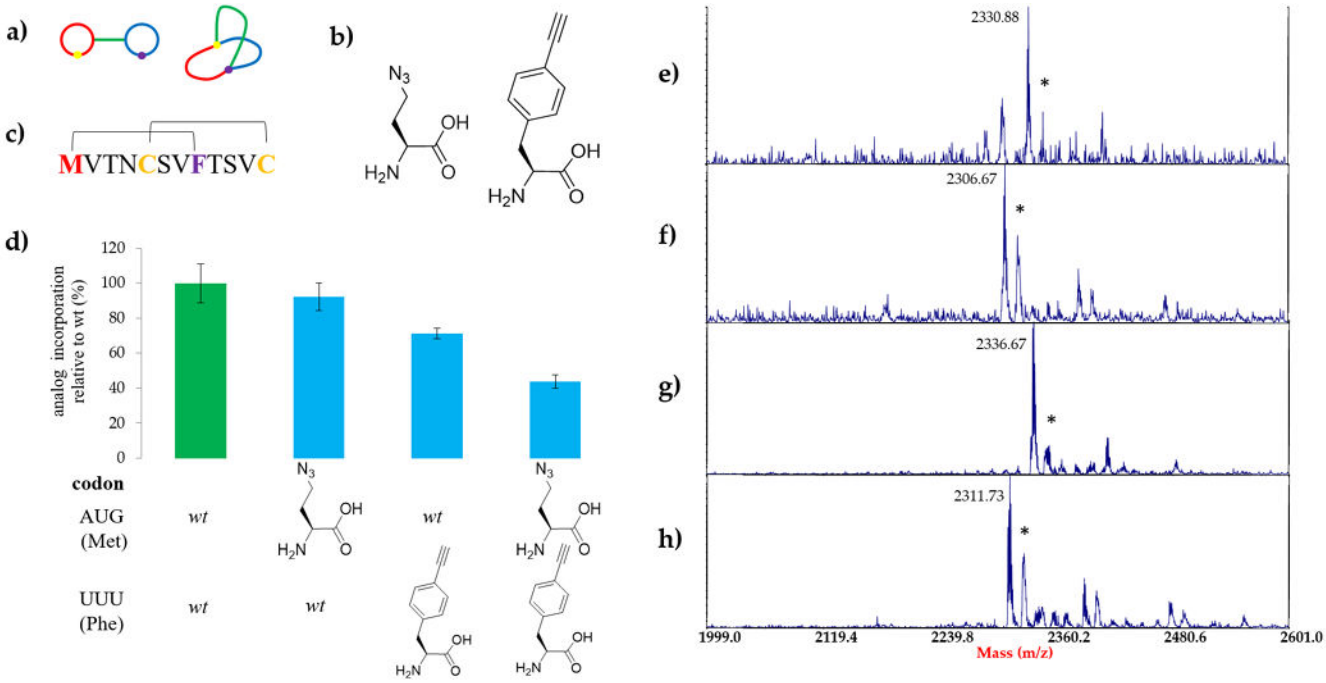

Figure 1. Scaffold conformations and analog incorporation

a) Bicyclic peptide conformations obtained from two orthogonal chemistries; manacle (left) and theta-bridged (right) b) Analogs β-azidohomoalanine (AzHA, left) and *p*-ethynyl phenylalanine (F-yne, right) incorporated in place of methionine and phenylalanine, respectively. c) Model peptide sequence, indicating the knotted-like theta conformation used for library design. d) Radiolabeled peptides were synthesized in sufficient quantities and MALDI-TOF confirmed appropriate mass for peptides containing e) both analogs (calc-2331.20), f) AzHA (calc-2306.98), g) F-yne (calc-2336.11), relative to h) All wild-type amino acids (calc-2311.97). * Indicates a ubiquitous +16 peak, presumably an artifact of sulfur oxidation during Zip-tip desalting.

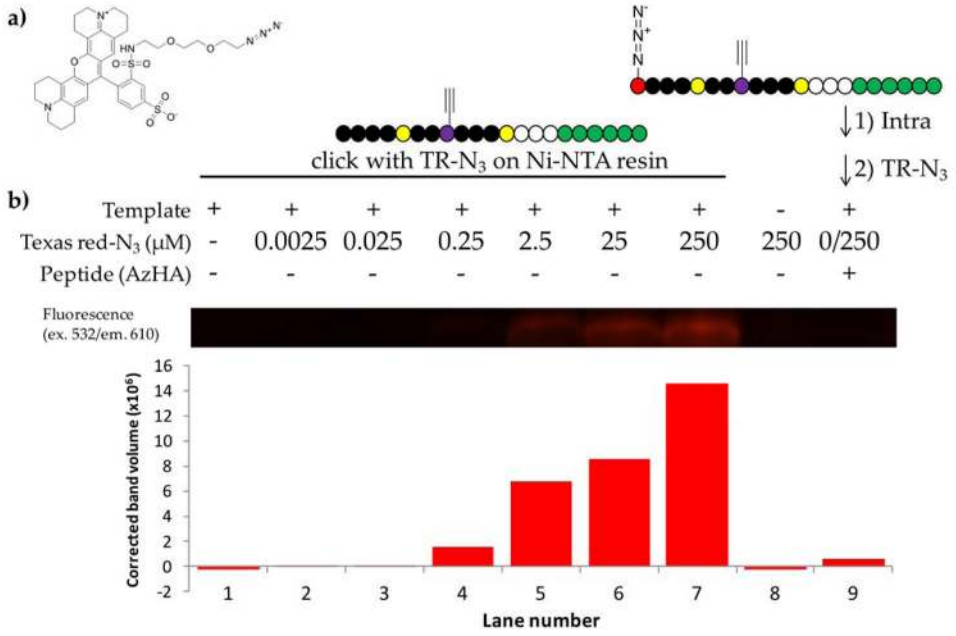

Figure 2. Click cyclization of peptides

a) Azide-functionalized sulfo-rhodamine-101 (Texas Red-azide or TR-N_3) used for fluorescent labeling. b) Concentration- dependent labeling of the (AzHA) peptide by TR-N_3. Negligible fluorescence is observed when the same reaction is performed on a 'pre-clicked' peptide containing both the azide and alkyne (far right lane), evidence that the intramolecular click cyclization has already occurred. Lanes 1–7: Concentration-dependent fluorescent labeling of alkyne-containing peptide with TR-N_3, indicating that the click reaction is compatible with Ni-NTA agarose-immobilized *in vitro* translated peptides. Lane 8: No mRNA template control reaction. Lane 9: TR-N_3 click-reacted with 'pre-clicked' azide/alkyne-containing peptide

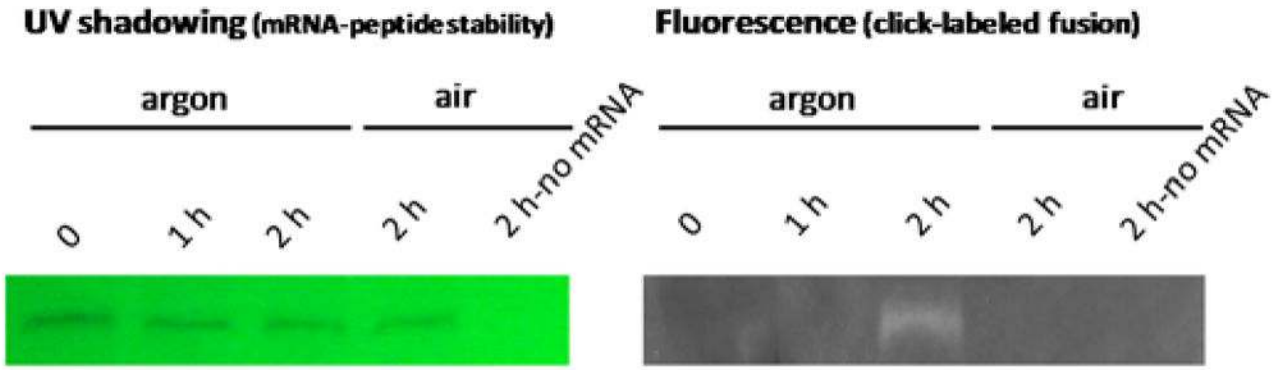

Figure 3. Click cyclization with mRNA-peptide fusions

Click reaction was performed with mRNA-(alkyne) peptide fusions immobilized on Ni-NTA resin and 250μM Texas Red-azide. Aliquots of beads were removed at the noted time points, fusions were washed and eluted with imidazole, and analyzed by 10% SDS-PAGE. Left, UV shadowing of mRNA-peptide fusion libraries over time. Right, Fluorescence image (ex 532, em 610) of the same gel.

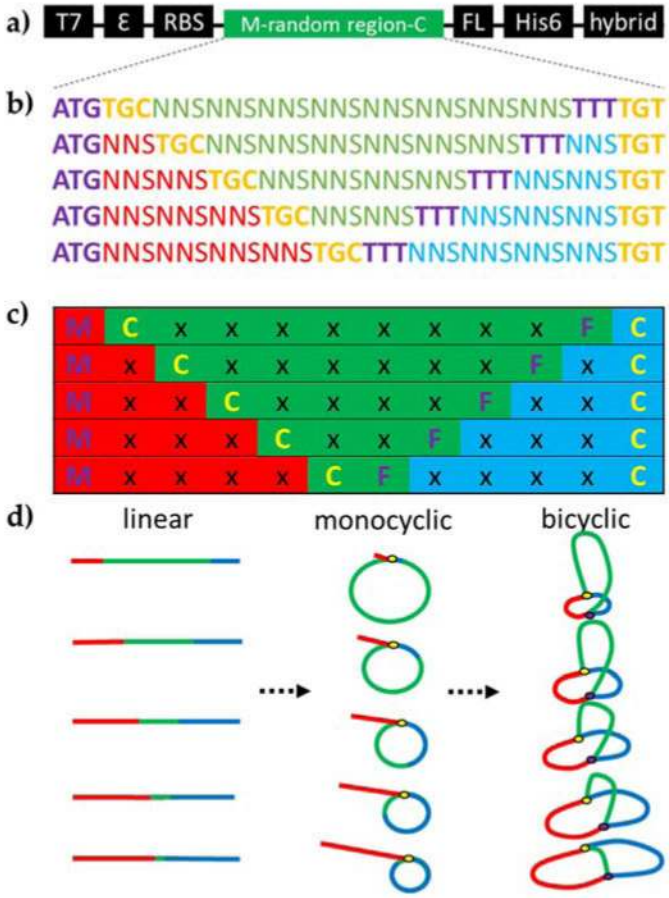

Figure 4. Design of cyclic libraries

a) General DNA library elements, b) Random library region construction, highlighting fixed 'clickable' codons in red and bisalkylatable cysteine codons in blue. c) Peptide sequences generated from the library mRNA (M = β-azidohomoalanine, F = *p*-ethynyl-phenylalanine, C = cysteine) d) Depictions of scaffold diversity generated from the linear mRNA fusions prepared by bisalkylation (monocyclic) and bisalkylation followed by CuAAC (bicyclic). The sequences are color coded as in (c). Yellow dots denote bis-alkylation cyclization, and purple dots represent CuAAC cyclization points.

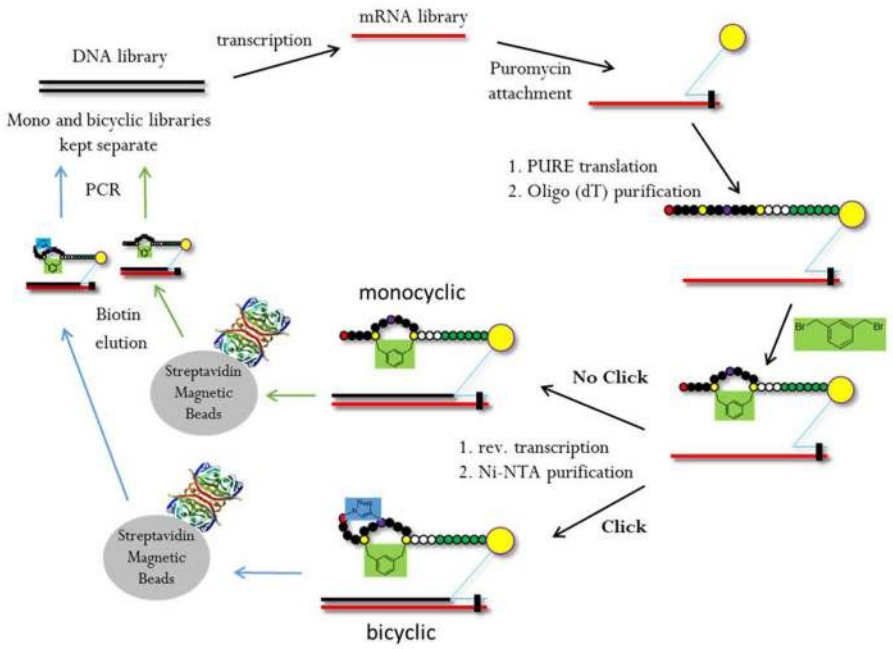

Figure 5. mRNA Display scheme

Comparative *in vitro* selections against streptavidin. PURE translation is initiated with puromycin-linked mRNA. mRNA-peptide fusions are bisalkylated with α,α′-dibromo-*m*-xylene (green box) while immobilized on oligo (dT) resin to form the monocyclic peptides. The monocyclic fusion pool is split after reverse transcription and bound to nickel resin, where the CuAAC reaction is performed on the portion of the pool targeted for bicyclic peptide formation (blue box). The monocyclic and bicyclic fusion pools are then used to select for high affinity binders to streptavidin. Following competitive elution with biotin, functional fusions were amplified via PCR to generate the enriched Round 2 DNA library. All steps were performed independently for subsequent rounds.

a)

	ClusterID		Rd 7			Rd 6			Rd 5			Rd 4	
			count	freq%	enrich	count	freq(%)	enrich	count	freq(%)	enrich	count	freq(%)
7.1m	1404	M T D P N C F G N P D C	4188	26.75	1.494	6026	17.91	3.87	6776	4.63	93.82	161	0.049
7.2m	1404	M T D P N C F G N P H C	3940	25.17	1.190	7114	21.14	3.01	10276	7.02	72.95	314	0.096
7.3m	1402	M T N P D C F G N P V C	3257	20.81	1.128	6845	20.35	3.55	10240	6.99	62.59	419	0.064
7.4m	1402	M T N P D C F A N P L C	447	2.86	1.058	908	2.70	2.23	1770	1.21	65.76	60	0.018
7.5m	1218	M T N P Q C F G N P Q C	210	1.34	0.673	671	1.99	1.77	1647	1.12	32.78	112	0.034
7.6m	1218	M T N P N C F G N P L C	188	1.20	0.946	427	1.27	1.85	1004	0.69	50.86	44	0.013
7.7m	1402	M T D P D C F G N P E C	112	0.72	0.652	369	1.10	1.42	1127	0.77	36.94	68	0.021
7.8m	1404	M T D P N C F G N P H C	108	0.69	1.080	215	0.64	2.58	363	0.25	38.53	21	0.006

b)

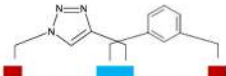

	ClusterID		Rd 9			Rd 8			Rd 7			Rd 6			Rd 5			Rd 4	
			count	freq(%)	enrich	count	freq(%)	enrich	count	freq(%)	enrich	count	freq(%)	enrich	count	freq(%)	enrich	count	freq(%)
9.1b	47984	M T D P N C F G N P D C	2191	1.96	5.31	1232	0.370	5.12	731	0.0722	6.935	32	0.0104	9.61	6	0.0011	3.58	4	0.00030
9.2b	47984	M T D P N C F G N P H C	1586	1.42	4.10	1154	0.346	4.85	723	0.0714	5.628	39	0.0127	8.79	8	0.0014	2.38	8	0.00061
9.3b	49379	M T N P D C F G N P V C	1290	1.15	4.33	1004	0.301	5.24	735	0.0725	3.698	53	0.0173	10.12	10	0.0018	2.15	10	0.00076
9.4b	39899	M **H P Q** N C F H V F S C	120	0.11	2.80	128	0.038	2.70	144	0.0142	1.749	25	0.0081	6.44	7	0.0013	16.68	1	0.00008
9.5lin	42373	M T I H Q W L Y **H P Q** C	79	0.07	33.67	7	0.002	5.32	4	0.0004	N/A	0	0.0000	N/A	0	0.0000	N/A	1	0.00008
9.6b	48929	M H P Y C F G F D N N C	62	0.06	9.25	20	0.006	3.38	18	0.0018	2.732	2	0.0007	3.61	1	0.0002	N/A	0	0.00000
9.7b	49379	M T N P D C F G N P A C	58	0.05	4.02	43	0.013	4.21	31	0.0031	N/A	0	0.0000	N/A	0	0.0000	N/A	0	0.00000
9.8b	49379	M T N P D C F A N P L C	40	0.04	3.98	30	0.009	3.26	28	0.0028	N/A	0	0.0000	0.00	1	0.0002	1.19	2	0.00015

Figure 6. AptaTOOLS round-by-round sequence analysis

Results of Illumina NextGen sequencing of a) rounds 4–7 of the monocyclic selection and b) rounds 4–9 of the bicyclic version. Round-by-round analysis includes tracking of the number of reads with that sequence (count), percentage of reads containing that sequence (freq %), and fold-increase in frequency from the previous round (enrich). Cluster ID denotes which Aptatools cluster the sequences were placed in. Highlighting indicates fixed flanking cyclization residues (red), intra-random region cyclization residues (aqua), and consensus residues within the random region (yellow). HPQ motif is in bold.

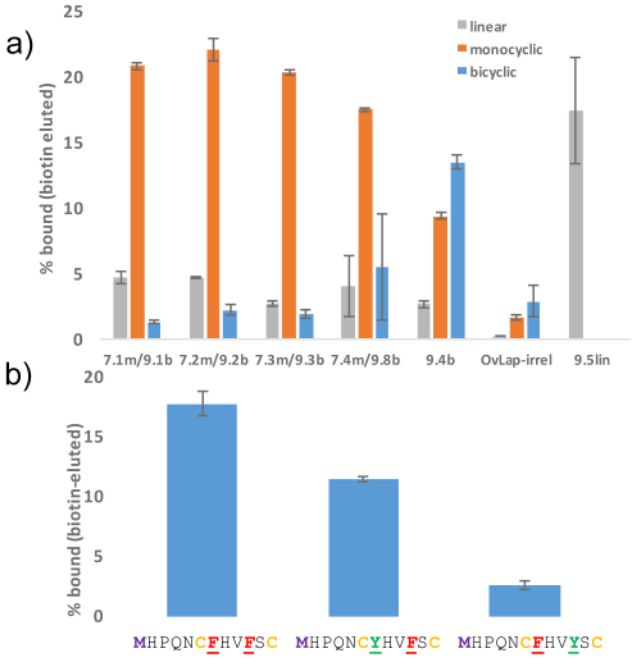

c)

scaffold	peptide	K_d (nM)
monocyclic	7.2m	361 ± 133
	7.3m	319 ± 98
bicyclic	9.4b	593 ± 62
	9.4b-7Y	568 ± 137

Figure 7. Binding to Strepdavidin

a) in vitro translated, 35S-Cys-labeled peptides were created in linear, monocyclic, and bicyclic conformations while immobilized on NI-NTA resin, bound to 1μM streptavidin beads and eluted with 2.5mM D-biotin. Model peptide (OvLap) was used as an irrelevant control and 9.5lin peptide was tested in only the linear form due to the absence of cyclizable residues. b) Selected bicyclic peptide 9.4b, with two F-yne residues (left). Tyrosine mutations to force the 10-member triazole cycle (middle) and the 7-member cycle (right). c) Binding affinities of the winners of the mono- and bicyclic selections.

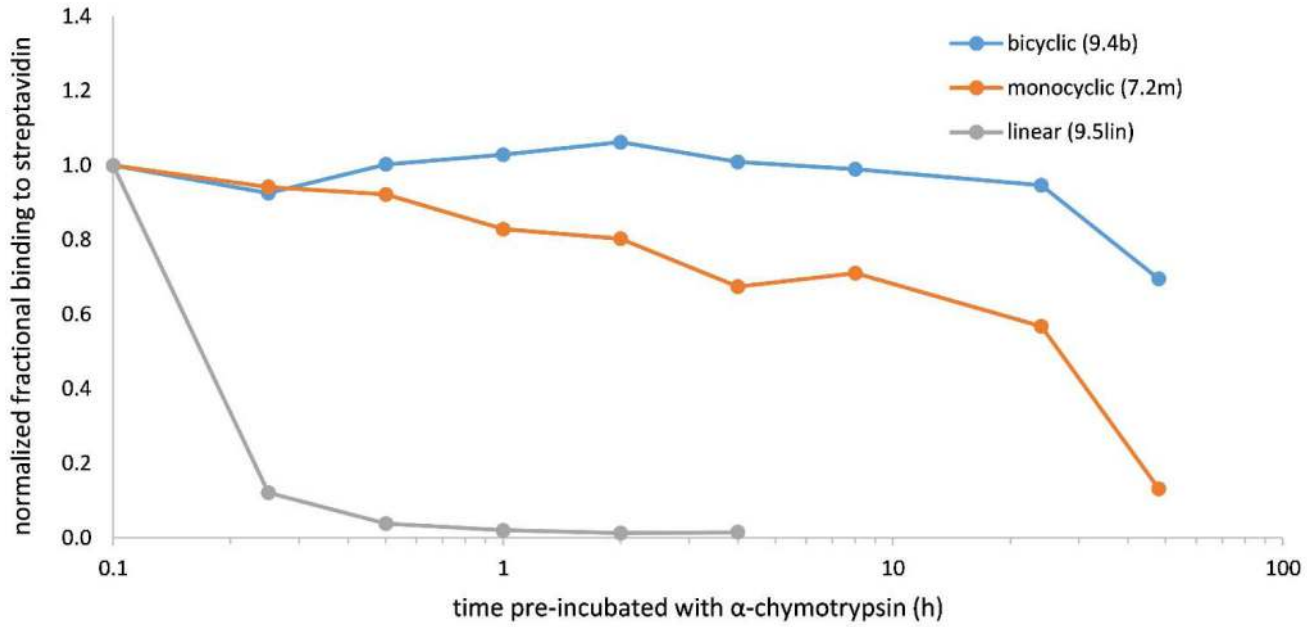

Figure 8. Protease stability

a) Normalized protease degradation of each of the three scaffolded peptides shown to bind streptavidin with the highest affinity (7.2m, 9.4b, 9.5lin). 5 nM peptide was added to 1.4U of immobilized α-chymotrypsin. Aliquots were removed at the indicated time points and added directly to 1 μM streptavidin beads, incubated for 2h, and eluted with biotin. Peptides were quantified by scintillation of ^{35}S-cysteine labeled peptides and normalized to the no protease time point. Results are an average of duplicate trials.